

**DEVELOPMENT OF HYBRID ORGANIC-
INORGANIC HYDRIDE FOR REVERSIBLE
HYDROGEN STORAGE**

TAN KHAI CHEN

UNIVERSITI SAINS MALAYSIA

2020

**DEVELOPMENT OF HYBRID ORGANIC-
INORGANIC HYDRIDE FOR REVERSIBLE
HYDROGEN STORAGE**

by

TAN KHAI CHEN

**Thesis submitted in fulfilment of the requirements
for the degree of
Master of Science**

May2020

ACKNOWLEDGEMENT

Thankfulness was woven into every aspect of my postgraduate studies life. First and foremost, I would like to dedicate my heartiest appreciation to my project supervisor, Dr. Chua Yong Shen for giving me an opportunity to carry out my Master degree under his supervision. I am extremely grateful to him for everything he did especially the knowledge and skill in developing hydrogen storage materials though he has busy schedule in the academic wise and researches. His dedication and keen interest above all his overwhelming attitude helps me in completing my research successfully.

I owe a deep sense of gratitude to Professor Dr. Chen Ping, Group Leader of Research Team 1901 in Dalian National Laboratory for Clean Energy for inviting me to join the research attachment via collaboration in Dalian, China for 10 months. Moreover, my delightful appreciation also goes to my co-supervisor, Professor Dr. He Teng, from Dalian National Laboratory for Clean Energy for his keen interest on assisting me at every stage of my research in Dalian. Although many obstacles had been faced, his prompt inspirations and timely suggestions with kindness have enabled me to carry out my research smoothly. Special thanks also go to Dr. Wu Anan, from Fujian Provincial Key Laboratory of Theoretical and Computational Chemistry, College of Chemistry and Chemical Engineering, Xiamen University and Dr. Wu Hui, from NIST Center for Neutron Research, National Institute of Standards and Technology, USA for their valuable contributions on thermodynamic calculations and first-principle calculations method for crystal structures, respectively.

Furthermore, it is my privilege to thank those postgraduate students (Pei Qijun, Yu Yang, Jing Zijun and Wang Jintao) from the laboratory at DICP for helping me no matter in terms of research project and life in Dalian. You guys are awesome! I would not forget to remember those researchers and officers from DICP who assisted me directly or indirectly.

Meanwhile, I would like to show my gratitude to the science officers and lab assistants (Mr. Megat, Mr. Kamarul, Mr. Mustaqim etc.) from Universiti Sains Malaysia (USM) for assisting and providing me instrumental supports. Special thanks to all my examiners whom provide me consecutive suggestions throughout my research. Not to forget, I would also like to acknowledge the financial support from USM Fellowship.

Last but not least, I am also very thankful to and fortunate enough to get constant encouragement and support from my parents, Mr. Tan Soon Lye and Mdm. Lee Kooi Choo. I am extremely fortunate to have this all along the completion of my project work. It would not have been possible without the kind support and help of my surrounding people.

Once again, thank you!

TABLE OF CONTENTS

ACKNOWLEDGEMENT	ii
TABLE OF CONTENTS	iv
LIST OF TABLES	vii
LIST OF FIGURES	ix
LIST OF SCHEMES	xiii
LIST OF SYMBOLS AND ABBREVIATIONS	xiiiv
LIST OF APPENDICES	xiii
ABSTRAK	xx
ABSTRACT	xxi
CHAPTER 1 INTRODUCTION	1
1.1 Background Study	1
1.2 Hydrogen Storage.....	2
1.3 Technologies for Hydrogen Storage	3
1.3.1 Liquified Hydrogen.....	4
1.3.2 Compressed Hydrogen.....	4
1.3.3 Hydrogen Storage in Solid Materials.....	6
1.4 Hydrogen Storage in Malaysia.....	8
1.5 Problem Statement	9
1.6 Research Objectives	10
CHAPTER 2 LITERATURE REVIEW	11
2.1 Physisorption Hydrogen Storage Materials.....	11
2.2 Chemisorption Hydrogen Storage Materials	13
2.2.1 Metal Hydrides.....	13
2.2.2 Alanates.....	15
2.2.3 Amide-Hydride Interaction	17

2.2.4	Borohydrides	21
2.2.5	Ammonia Borane and Metal Amidoborane	21
2.2.6	Organic Hydrides	23
	2.2.6(a) Catalytic Hydrogenation and Dehydrogenation Reactions	29
CHAPTER 3 METHODOLOGY.....		30
3.1	Chemicals	30
3.2	Instrumentation and Characterization Techniques	31
3.2.1	Solid State Ball-milling.....	31
3.2.2	X-ray Diffraction (XRD) Analysis	32
3.2.3	Nuclear Magnetic Resonance (NMR) Spectroscopic Analysis	32
3.2.4	Thermogravimetric Analysis (TGA).....	33
3.3	Experimental Section	33
3.3.1	Syntheses of Metalorganic Hydrides	33
3.3.2	Hydrogen Absorption and Desorption of Metalorganic Hydrides.	36
3.3.3	Thermodynamic and Chemical Shift Calculations	36
3.3.4	First-principle Calculations Method for Crystal Structures.....	37
3.3.5	<i>Quasi In-situ</i> Nuclear Magnetic Resonance (NMR).....	38
CHAPTER 4 RESULTS AND DISCUSSION		39
4.1	Thermodynamic Calculations	39
4.2	Syntheses and Crystal Structures of Metalorganic Hydrides	48
4.3	Hydrogen Absorption and Desorption	61
4.4	Synthesis of Metallo-Carbazolide Using Different Alkali Metal-based Precursors	68
4.5	<i>Quasi In-situ</i> NMR Study on Pristine Carbazole and Sodium Hydride.....	81
CHAPTER 5 CONCLUSION AND RECOMMENDATION		85
5.1	Conclusion.....	85
5.2	Recommendation.....	86

REFERENCES..... 88

APPENDICES

**LIST OF PUBLICATIONS, CONFERENCE PRESENTATIONS AND
INNOVATIONS**

LIST OF TABLES

	Page
Table 1.1	Mass energy densities for different fuels2
Table 1.2	DOE targets for onboard hydrogen storage systems for light-duty vehicles.....3
Table 1.3	Comparison between physisorption and chemisorption from various aspects8
Table 2.1	Physical constants of selected complex aluminium hydrides 17
Table 2.2	Summary of the chemical reactions of metal-N-H hydrogen storage systems20
Table 2.3	Examples of different cycloalkanes with their enthalpies of dehydrogenation.....24
Table 2.4	Examples of heterocyclic aromatic compounds with their hydrogen storage capacity and enthalpy of reaction25
Table 2.5	Thermodynamic data per H ₂ molecule liberated from selected organic compounds proposed by Clot et al. (unit for ΔH_d and ΔG_d = kcal mol ⁻¹ ; ΔS_d = cal mol ⁻¹ K ⁻¹ ; T _d = K), where T _d is the temperature corresponding to $\Delta G_d = 0$26
Table 2.6	Examples of heterogenous catalysts with its components used in reversible hydrogenation and dehydrogenation29
Table 3.1	List of Chemicals30
Table 4.1	Hydrogen storage capacity and enthalpy of dehydrogenation (ΔH_d) of N-heterocycles and metallo-N-heterocycles, (M = Li, Na, K, Mg, Ca).....44
Table 4.2	Calculated results on metallo-pyrrolide/tetrahydropyrrolide with X1s method45
Table 4.3	Calculated results on metallo-imidazolide/tetrahydroimidazolide with X1s method46

Table 4.4	Calculated results on metallo-carbazolide/dodecahydrocarbazolide with X1s method	47
Table 4.5	The average values of C-H bond length of metallo-dodecahydrocarbazole (Å)	48
Table 4.6	Crystallographic data of the DFT relaxed structure of Na-pyrrolide	59
Table 4.7	Crystallographic data of the DFT relaxed structure of Na-imidazolide.....	60
Table 4.8	Cell parameters of the refined structures of metallated N-heterocycles.....	60
Table 4.9	Interatomic bond distances (Å) comparison of Na-pyrrolide DFT relaxed structure and pristine pyrrole.....	60
Table 4.10	Interatomic bond distances (Å) comparison of Na-imidazolide DFT relaxed structure and pristine imidazole.....	60
Table 4.11	Dehydrogenation of dodecahydrocarbazole and lithium dodecahydrocarbazolide by employing various supported noble metal catalysts at 200 °C.....	67

LIST OF FIGURES

	Page
Figure 1.1	Petroleum consumption from 1949 to 2011 in USA from different sectors..... 1
Figure 1.2	Volumetric density of compressed hydrogen gas as a function of gas pressure in comparison with the ideal gas and liquid hydrogen5
Figure 1.3	(a) Physisorption and (b) chemisorption of hydrogen on solid materials 7
Figure 2.1	Pressure-concentration-temperature plot and a van't Hoff curve 15
Figure 2.2	PCT curve of $\text{Li}_2\text{Mg}(\text{NH})_2$ at 180 °C..... 19
Figure 2.3	Crystal structure of ammonia borane 22
Figure 2.4	Structural formula of N-ethylcarbazole (left) and carbazole (right) ..27
Figure 2.5	Structural formula of (a) pyrrole and (b) imidazole.....28
Figure 4.1	Proposed reactions for reversible hydrogen storage using metallo-N-heterocycles. *For the ease of illustration, M in (a) is monovalent40
Figure 4.2	ΔH_d of different metallo-N-heterocycles versus electronegativities of H and metals40
Figure 4.3	ΔH_d versus the charge transfer from metal to aromatic rings41
Figure 4.4	The length of C-H at α site of M-H-CZ versus electronegativities of H and metals41
Figure 4.5	XRD patterns of sodium and lithium analogues of pyrrolides.....49
Figure 4.6	XRD patterns of sodium and lithium analogues of imidazolides49
Figure 4.7	XRD patterns of sodium and lithium analogues of carbazolides.....50
Figure 4.8	^1H NMR spectra of synthesized metallo-pyrrolides as compared to its molecular counterpart in <i>d</i> -DMSO.....51

Figure 4.9	^{13}C NMR spectra of synthesized metallo-pyrrolides as compared to its molecular counterparts in <i>d</i> -DMSO	51
Figure 4.10	^1H NMR spectra of synthesized metallo-carbazolides as compared to its molecular counterpart in <i>d</i> -DMSO.....	52
Figure 4.11	^{13}C NMR spectra of synthesized metallo-carbazolides as compared to its molecular counterpart in <i>d</i> -DMSO.....	52
Figure 4.12	Simulated ^{13}C NMR of pyrrole (left) and sodium pyrrolide (right) in DMSO	53
Figure 4.13	Simulated ^{13}C NMR of carbazole (left) and sodium carbazolidide (right) in DMSO.....	54
Figure 4.14	^7Li NMR spectra of synthesized metallated pyrrolide and carbazolidide	54
Figure 4.15	^{23}Na NMR spectra of synthesized metallated pyrrolide and carbazolidide	55
Figure 4.16	Experimental (circles), fitted (line), and difference (line below observed and calculated patterns) XRD profiles (CuK α radiation) for Na-imidazolide ($\text{NaC}_3\text{H}_3\text{N}_2$) at 298 K. Vertical bars indicate the calculated positions of Bragg peaks	56
Figure 4.17	Experimental (circles), fitted (line), and difference (line below observed and calculated patterns) XRD profiles (CuK α radiation) for Na-pyrrolide ($\text{NaC}_4\text{H}_4\text{N}$) at 298 K. Vertical bars indicate the calculated positions of Bragg peaks. An extra peak at 9.965° from an unknown impurity phase was excluded in the pattern	57
Figure 4.18	Crystal structures (left) and local coordination of Na^+ cation (right) of sodium imidazolide. Blue sphere: nitrogen, green sphere: sodium, black sphere: carbon and pink sphere: hydrogen.....	58
Figure 4.19	Crystal structures (left) and local coordination of Na^+ cation (right) of sodium pyrrolide. Blue sphere: nitrogen, green sphere: sodium, black sphere: carbon and pink sphere: hydrogen	59

Figure 4.20	Hydrogen absorption of Li-CZ at 7 MPa over different catalysts: (1) Li-CZ and Ru metal with molar ratio 2.8:1 at 100 °C, (2) to (5) Li-CZ and Ru, Pd, Pt, Rh metals with molar ratio 5:1 at 200 °C	62
Figure 4.21	¹ H NMR spectra of hydrogenated lithium carbazolidine at 200 °C (70 bar) employing various unsupported noble metal catalysts (ratio 1:5) in <i>d</i> -DMSO.....	63
Figure 4.22	¹³ C NMR spectra of hydrogenated lithium carbazolidine at 200 °C (70 bar) employing various unsupported noble metal catalysts (ratio 1:5) in <i>d</i> -DMSO.....	63
Figure 4.23	Conversion of lithium carbazolidine catalyzed by Ru particles.....	64
Figure 4.24	¹ H NMR spectra of the neat and hydrogenated lithium carbazolidine by employing Ru particles (ratio 1:2.8) in <i>d</i> -DMSO.....	64
Figure 4.25	¹³ C NMR spectra of the neat and hydrogenated lithium carbazolidine by employing Ru particles (ratio 1:2.8) in <i>d</i> -DMSO.....	65
Figure 4.26	Measurement on the heat of hydrogenation of lithium carbazolidine using C80	66
Figure 4.27	¹ H NMR spectra of the neat lithium carbazolidine and the dehydrogenated lithium dodecahydrocarbazolidines catalyzed by Pd/C and Rh/Al ₂ O ₃ at 200 °C	67
Figure 4.28	TPD-MS of the syntheses of metallo-carbazolidines using lithium hydride.....	70
Figure 4.29	TPD-MS of the syntheses of metallo-carbazolidines using sodium hydride.....	71
Figure 4.30	TGA of post-milled pristine carbazole with lithium hydride after heated up to ~400 °C.....	71
Figure 4.31	TGA of post-milled pristine carbazole with sodium hydride after heated up to ~400 °C.....	72
Figure 4.32	Hydrogen release upon the heat treatment of ball milled LiH- carbazole at 250 °C	72

Figure 4.33	Hydrogen release upon the heat treatment of ball milled NaH-carbazole at 243 °C	73
Figure 4.34	TPD-MS of the syntheses of metallo-carbazolides using lithium amide	73
Figure 4.35	TPD-MS of the syntheses of metallo-carbazolides using sodium amide	74
Figure 4.36	TGA of post-milled pristine carbazole with sodium amide after heated up to ~400 °C.....	74
Figure 4.37	TGA of pristine carbazole after heated up to ~400 °C.....	75
Figure 4.38	XRD of lithium carbazolidide using different metal-based compounds as metal precursors	76
Figure 4.39	XRD of sodium carbazolidide using different metal-based compounds as metal precursors	76
Figure 4.40	(a) ¹ H NMR of metallo-carbazolides as compared to pristine carbazole in DMSO- <i>d</i> ₆ . (b) Enlargement of ¹ H NMR of metallo-carbazolides spectrum from the range 6.5 to 8.5 ppm	78
Figure 4.41	¹³ C NMR of metallo-carbazolides as compared to pristine carbazole in DMSO- <i>d</i> ₆	79
Figure 4.42	⁷ Li NMR of lithium and sodium carbazolidide.....	80
Figure 4.43	²³ Na NMR of lithium and sodium carbazolidide	80
Figure 4.44	<i>Quasi in situ</i> ¹ H NMR of sodium carbazolidide by gradually increasing the percentage of using sodium hydride as compared to pristine carbazole in DMSO- <i>d</i> ₆	83
Figure 4.45	Calculated ¹ H NMR of carbazole DMSO	83
Figure 4.46	Calculated ¹ H NMR of Na ⁺ -carbazole in DMSO	84
Figure 4.47	Calculated ¹ H NMR of carbazolidide anion in DMSO.....	84

LIST OF SCHEMES

	Page
Scheme 2.1 Interaction between lithium amide and lithium hydride to form lithium imide and H ₂	18
Scheme 3.1 Synthetic pathway of metalorganic hydrides using lithium and sodium hydride. *where M ⁿ , with n = +1. In case of n = +2, it is expected that above equations remain valid with twice as much anions (pyrrolide, imidazolide or carbazolide) and hydrogen will be liberated	35
Scheme 3.2 Synthetic pathway of metalorganic hydrides using metal amides. *where M ⁿ , with n = +1	36

LIST OF SYMBOLS AND ABBREVIATIONS

°	Degree
°C	Degree Celsius
MJ kg ⁻¹	Mega Joule per kilogram
MJ L ⁻¹	Mega Joule per litre
kg m ⁻³	Kilogram per cubic metre
K	Kelvin
km	Kilometre
kWh/kg	Kilowatt-hour per kilogram
kWh/L	Kilowatt-hour per litre
min.	Minimum
max.	Maximum
kJ mol ⁻¹	Kilo Joule per mole
CO ₂	Carbon dioxide
COP	Conference of the Parties
¹ H NMR	Proton nuclear magnetic resonance
¹³ C NMR	Carbon-13 nuclear magnetic resonance
⁷ Li NMR	Lithium-7 nuclear magnetic resonance
²³ Na NMR	Sodium-23 nuclear magnetic resonance
wt%	Weight percent
cm ³ g ⁻¹	Cubic centimetre per gram
m ² g ⁻¹	Metre square per gram
nm	Nanometre
Å	Angstrom, 1 × 10 ⁻¹⁰ m
kg cm ⁻³	Kilogram per cubic centimetre
ΔH	Enthalpy changed

ΔH_d	Enthalpy changed of dehydrogenation
ΔS	Entropy changed
P°	Reference pressure at atmospheric pressure
P	Equilibrium pressure
R	Gas constant
T	Absolute temperature
Ti	Titanium
Nb	Columbium
V	Vanadium
Mn	Manganese
Fe	Iron
Co	Cobalt
Ni	Nickel
In	Indium
NaAlH_4	Sodium aluminium hydride
TiCl_3	Titanium (III) chloride
Na_3AlH_6	Trisodium aluminium hexahydride
Al	Aluminium
Na	Sodium
LiAlH_4	Lithium aluminium hydride
Li_3AlH_6	Trilithium aluminium hexahydride
<i>ca.</i>	Circa
Ref.	Reference
>	Greater than
Li_3N	Lithium nitride
Li_2NH	Lithium imide
$\text{H}^{\delta+}$	Protic hydrogen

H ^{δ-}	Hydridic hydrogen
et al.	And others
Li ₂ O	Lithium oxide
kg H ₂ L ⁻¹	1 litre of hydrogen weigh (in kilogram)
g H ₂ L ⁻¹	1 litre of hydrogen weigh (in gram)
mm	Millimetre
Tr	Terbium
SBA-15	Santa Barbara Amorphous-15
MCM-41	Mobil Composition Matter-41
CO	Carbon monoxide
N	Nitrogen
ΔG	Change of Gibbs energy
K ₂ O	Potassium oxide
MgO	Magnesium oxide
Cu	Copper
MoO ₂	Molybdenum dioxide
MoS ₂	Molybdenum disulfide
SiO ₂	Silicon dioxide
TPD-MS	Temperature Programmed Desorption-Mass Spectroscopy
DMSO	Dimethylsulfoxide
XRD	X-ray Diffraction
s	Second
min	Minute
λ	Lambda
kV	Kilovolt
mA	Milliampere
mg	Milligram

g	Gram
h	Hour
μL	microlitre
rpm	Revolutions per minute
$^{\circ}\text{C min}^{-1}$	Degree Celsius per minute
~	Approximate
mL	Millilitre
TMS	Tetramethylsilane
GGA	Generalized gradient approximation
meV	Mega electron-volt
eV \AA^{-1}	Electron-volt per Angstrom
NBO	Natural bond orbital
ps	picosecond
%	percent
\geq	Greater than or equal to
OH	Hydroxide
NH_2	Amine
tot	Total
R_{wp}	Weighted powder profile R-factor
R_{p}	Ruddlesden-popper
\approx	Near to
NH_3	Ammonia
TGA	Thermogravimetric analysis
ppm	Part per million
kV	Kilovolt
THF	Tetrahydrofuran

LIST OF APPENDICES

- APPENDIX 1 THERMODYNAMIC CALCULATION (PYRROLE)
- APPENDIX 2 THERMODYNAMIC CALCULATION (MG-PYRROLIDE)
- APPENDIX 3 THERMODYNAMIC CALCULATION (CA-PYRROLIDE)
- APPENDIX 4 THERMODYNAMIC CALCULATION (LI-PYRROLIDE)
- APPENDIX 5 THERMODYNAMIC CALCULATION (NA-PYRROLIDE)
- APPENDIX 6 THERMODYNAMIC CALCULATION (K-PYRROLIDE)
- APPENDIX 7 THERMODYNAMIC CALCULATION (TETRAHYDROPYRROLE)
- APPENDIX 8 THERMODYNAMIC CALCULATION (MG-TETRAHYDROPYRROLIDE)
- APPENDIX 9 THERMODYNAMIC CALCULATION (CA-TETRAHYDROPYRROLIDE)
- APPENDIX 10 THERMODYNAMIC CALCULATION (LI-TETRAHYDROPYRROLIDE)
- APPENDIX 11 THERMODYNAMIC CALCULATION (NA-TETRAHYDROPYRROLIDE)
- APPENDIX 12 THERMODYNAMIC CALCULATION (K-TETRAHYDROPYRROLIDE)
- APPENDIX 13 THERMODYNAMIC CALCULATION (IMIDAZOLE)
- APPENDIX 14 THERMODYNAMIC CALCULATION (MG-IMIDAZOLIDE)
- APPENDIX 15 THERMODYNAMIC CALCULATION (CA-IMIDAZOLIDE)
- APPENDIX 16 THERMODYNAMIC CALCULATION (LI-IMIDAZOLIDE)
- APPENDIX 17 THERMODYNAMIC CALCULATION (NA-IMIDAZOLIDE)
- APPENDIX 18 THERMODYNAMIC CALCULATION (K-IMIDAZOLIDE)
- APPENDIX 19 THERMODYNAMIC CALCULATION (TETRAHYDROIMIDAZOLE)
- APPENDIX 20 THERMODYNAMIC CALCULATION (MG-TETRAHYDROIMIDAZOLIDE)
- APPENDIX 21 THERMODYNAMIC CALCULATION (CA-TETRAHYDROIMIDAZOLIDE)
- APPENDIX 22 THERMODYNAMIC CALCULATION (LI-TETRAHYDROIMIDAZOLIDE)

APPENDIX 23	THERMODYNAMIC CALCULATION (NA-TETRAHYDROIMIDAZOLIDE)
APPENDIX 24	THERMODYNAMIC CALCULATION (K-TETRAHYDROIMIDAZOLIDE)
APPENDIX 25	THERMODYNAMIC CALCULATION (CARBAZOLE)
APPENDIX 26	THERMODYNAMIC CALCULATION (MG-CARBAZOLIDE)
APPENDIX 27	THERMODYNAMIC CALCULATION (CA-CARBAZOLIDE)
APPENDIX 28	THERMODYNAMIC CALCULATION (LI-CARBAZOLIDE)
APPENDIX 29	THERMODYNAMIC CALCULATION (NA-CARBAZOLIDE)
APPENDIX 30	THERMODYNAMIC CALCULATION (K-CARBAZOLIDE)
APPENDIX 31	THERMODYNAMIC CALCULATION (DODECAHYDROCARBAZOLE)
APPENDIX 32	THERMODYNAMIC CALCULATION (MG-DODECAHYDROCARBAZOLIDE)
APPENDIX 33	THERMODYNAMIC CALCULATION (CA-DODECAHYDROCARBAZOLIDE)
APPENDIX 34	THERMODYNAMIC CALCULATION (LI-DODECAHYDROCARBAZOLIDE)
APPENDIX 35	THERMODYNAMIC CALCULATION (NA-DODECAHYDROCARBAZOLIDE)
APPENDIX 36	THERMODYNAMIC CALCULATION (K-DODECAHYDROCARBAZOLIDE)

PEMBANGUNAN HIBRID ORGANIK-TAK ORGANIK HIDRIDA UNTUK PENYIMPANAN HIDROGEN BERBALIK

ABSTRAK

Menyimpan hidrogen dengan efisien dalam bahan berfasa cecair dan pepejal adalah cabaran utama dalam isu penyimpanan hidrogen. Kebanyakan usaha telah diberi kepada hidrida tak organik yang mengandungi ikatan B-H, Al-H dan/atau N-H, sementara sebatian organik yang mempunyai pelbagai ikatan yang mudah dimanipulasi kurang diberi perhatian atas sebab sifat termodinamik dan kepilihan hasil pendehidrogenan yang kurang memuaskan. Oleh hal yang demikian, kami membangunkan sejenis bahan penyimpanan hidrogen baru yang merangkumi sebatian tak organik dan organik, iaitu logam N-heterosikel, menggunakan sifat pendermaan elektron logam alkali bagi melaraskan kekuatan ikatan C-H, C-N dan C-C dalam molekul N-heterosikel dan seterusnya sifat termodinamik pendehidrogenannya supaya bersesuaian dengan aplikasi penyimpanan hidrogen. Pengiraan teori mendedahkan bahawa entalpi pendehidrogenan (ΔH_d) daripada logam N-heterosikel dipengaruhi oleh keelektronegatifan logam. Selaras dengan keputusan pengiraan, analog natrium dan lithium daripada pirolida, imidazolida, dan karbazolida yang menunjukkan struktur yang baru telah berjaya disintesis dan diciri untuk kali pertama, di mana interaksi kation- π telah dikenalpasti. Lebih penting lagi, penyerapan dan penyaherapan hidrogen berbalik boleh dicapai melalui litium karbazolida yang mempunyai kapasiti hidrogen setinggi 6.5 wt% dan entalpi pendehidrogenan yang sesuai iaitu $34.2 \text{ kJ mol}^{-1}\text{-H}_2$.

DEVELOPMENT OF HYBRID ORGANIC-INORGANIC HYDRIDE FOR REVERSIBLE HYDROGEN STORAGE

ABSTRACT

Storing hydrogen efficiently in condensed materials is a key technical challenge. Tremendous efforts have been given to inorganic hydrides containing B-H, Al-H and/or N-H bonds, while organic compounds with a great variety and rich chemistry in manipulating C-H and unsaturated bonds, however, are undervalued mainly because of their unfavourable thermodynamics and selectivity in dehydrogenation. Here, we developed a new family of hydrogen storage material spanning across the domain of inorganic and organic hydrogenous compounds, namely metallo-N-heterocycles, utilizing the electron donating nature of alkali or alkaline earth metals to tune the strengths of C-H, C-N and C-C bonds of N-heterocyclic molecules to be suitable for hydrogen storage in terms of thermodynamic and kinetic properties. Theoretical calculations reveal that the enthalpies of dehydrogenation (ΔH_d) of these metallo-N-heterocycles are dependent on the electronegativity of the metals. In line with our calculation results, sodium and lithium analogues of pyrrolides, imidazolides and carbazolides of distinct structures were synthesized and characterized for the first time, where the cation- π interaction was identified. More importantly, a reversible hydrogen absorption and desorption can be achieved over lithium carbazolidide which has a hydrogen capacity as high as 6.5 wt% and a suitable enthalpy of dehydrogenation of 34.2 kJ mol⁻¹-H₂ for on-board hydrogen storage.

CHAPTER 1

INTRODUCTION

1.1 Background Study

Department of Energy (DOE) of United State in 2011 proclaimed that transportation in USA dissipates more than half of petroleum in the past decades¹. Moreover, non-renewable fossil fuel is finite and thus will eventually be used up. From the environmental impact point of view, transportation using petroleum based fuel (gasoline or diesel) imposes several environmental effects. One of these major effects is global warming, which is a consequence of uncontrolled emission of carbon dioxide². Other than that, exhaustion of carbon monoxide, nitrogen oxides and sulfur oxides from the burning of petroleum may also lead to negative impacts on both public health and ecosystem³. As such, in order to achieve a more sustainable developed society in the twenty-first century, an alternative source of energy should be used to replace contemporary fossil fuel. The consumption of petrol estimated by different sectors in USA from 1949 to 2011 is exhibited in Figure 1.1.

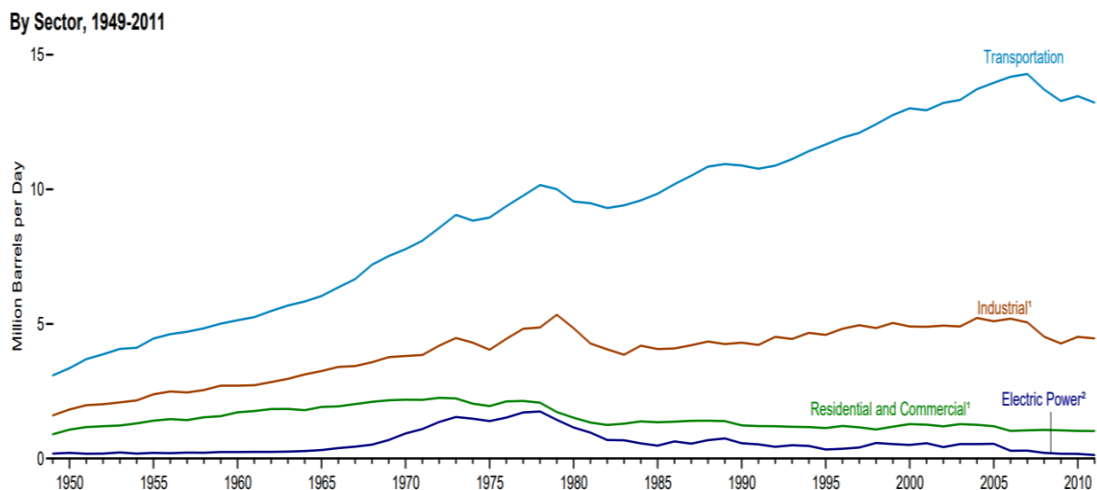


Figure 1.1: Petroleum consumption from 1949 to 2011 in USA from different sectors¹.

Hydrogen has been getting attention lately to become one of the best potential sources to replace conventional energy due to several advantages: 1) Hydrogen is present abundantly in nature. 2) The mass density of hydrogen is of paramount higher than other common fuels⁴. 3) Production of water as the only product and 4) The hydrogen fuel cell efficiency which is of fundamental importance is 3 times more efficient⁵. Table 1.1 below reveals the mass energy densities for different fuels adopted from DOE in 2011.

Table 1.1: Mass energy densities for different fuels¹.

Fuel	Hydrogen weight fraction	Ambient state	Mass energy (MJ kg ⁻¹)
Hydrogen	1.00	Gas	120
Methane	0.25	Gas	50 (43) ²
Ethane	0.20	Gas	47.5
Propane	0.18	Gas (liquid) ¹	46.4
Gasoline	0.16	Liquid	44.4
Ethanol	0.13	Liquid	26.8
Methanol	0.12	Liquid	19.9

¹A gas at room temperature, but normally stored as a liquid at moderate pressure.

²The larger the values are for pure methane. The values in parentheses are for a 'typical' natural gas.

1.2 Hydrogen Storage

Although hydrogen can be used as the current source of energy, the highly explosive nature of hydrogen demands a safe and practical hydrogen storage system for the purpose of achieving global introduction of hydrogen fuel cells⁶. In the past, storing enough hydrogen on-board a vehicle for an average driving distance of 300 miles was one the greatest challenges and it is impractical as compared to current gasoline vehicles⁷. Referring to Table 1.1 above, hydrogen possesses the highest gravimetric densities compared to the rest of known fuels. However, the volumetric energy densities of liquid hydrogen (8 MJ L⁻¹) are significantly lower as compared to that of gasoline (32 MJ L⁻¹), indicating a great challenge to store hydrogen compactly for vehicular application.

In the early stage, the intention of setting up targets for onboard hydrogen storage systems for light-duty vehicles has caused DOE in 2009 to establish a partnership with the U.S DRIVE, the U.S. Council for Automotive Research, and major energy and utility companies⁸. The main objective of setting up this target is to fulfil packaging, cost, safety and performance requirements to be competitive with comparable vehicles in the market place⁹. Eventually, a list of targets for light-duty vehicles onboard hydrogen storage was developed by DOE⁸. Table 1.2 shows the primary DOE target for on board hydrogen storage. To achieve a driving range of 300 miles (500 km) for light duty vehicles, a system capacity with gravimetric and volumetric densities of 1.8 kWh/kg and 1.3 kWh/L, respectively, are required. In addition, the hydrogen delivery temperatures should fall in the range of -40 to 85 °C. If the temperature requirement is expressed in the form of reaction enthalpy, the enthalpy of dehydrogenation of the system targeted by DOE ranges from 26 kJ mol⁻¹ to 40 kJ mol⁻¹-H₂. Undeniably, when developing systems for hydrogen storage, all targets shown in Table 1.2 need to be primarily taken into consideration.

Table 1.2: DOE targets for onboard hydrogen storage systems for light-duty vehicles⁸.

Storage Parameter		Units	2020	2025	Ultimate
System capacity	gravimetric	kWh/kg (kg H ₂ /kg system)	1.5 (0.045)	1.8 (0.055)	2.2 (0.065)
System capacity	volumetric	kWh/L (kg H ₂ /L system)	1.0 (0.030)	1.3 (0.040)	1.7 (0.050)
Hydrogen temperature (min. /max.)	delivery	° C	-40/85	-40/85	-40/85
Operating pressure (min. /max.) fuel cell		bar	5/12	5/12	5/12

1.3 Technologies for Hydrogen Storage

The criteria to develop an effective hydrogen storage technology for application in transportation includes high storage capacity, optimum operating temperature, and fast kinetics¹⁰. Up to present, there are three types of technologies

accessible to store the hydrogen including compressing hydrogen, liquefying hydrogen and hydrogen storage in solid materials¹¹. Empirically, storing hydrogen in solid materials is achieved through two different processes: physisorption and chemisorption. Physical adsorption is defined as a process in which the hydrogen is adsorbed on the surface of solid materials whereas chemisorption involves the reaction of hydrogen reacts with the solid materials to form chemical bonds⁹.

1.3.1 Liquefied Hydrogen

In general, decreasing the temperature of hydrogen gas at a constant pressure will cause the liquefaction of the hydrogen gas to occur¹². According to Ahluwalia and Peng¹³⁻¹⁴, a liquid hydrogen container can be filled on-board the vehicle in just 3 minutes. Because liquid hydrogen possesses a density of about 80 kg m^{-3} at 22 K and a pressure of 4 bar, therefore when compared to compressed hydrogen, the volume would be required for liquefied hydrogen storage is somehow lower than that¹⁵.

However, there are also several obstacles faced when dealing with liquefied hydrogen storage such as huge energy requirement for hydrogen liquefaction, hydrogen boil-off and tank cost⁹. By way of illustration, the boiling point of hydrogen at ambient pressure is 20 K, in which at this temperature, most of the gases are in solid state¹². As such, in order to maintain hydrogen as liquid state and to avoid hydrogen from being vaporized, the implementation of cooling equipment¹⁶ and strong thermal insulators¹² should be included. As such, the weights and volumes of such equipment must be considered upon the design of the storage system.

1.3.2 Compressed Hydrogen

Among all the technologies discussed earlier, storing hydrogen in compressed form provides the easiest and simplest way. From Figure 1.2, a deviation of

hydrogen gas took place from the ideal gas, typically at high pressure. Fundamentally, hydrogen gas follows an ideal gas law, in which at constant temperature, increasing the pressure of gas will reduce the gas volume and thus improve the gas volumetric density¹¹. However, when comparing this statement to the Figure 1.2 below, the curve deviates from the ideal gas law especially when the pressure is high.

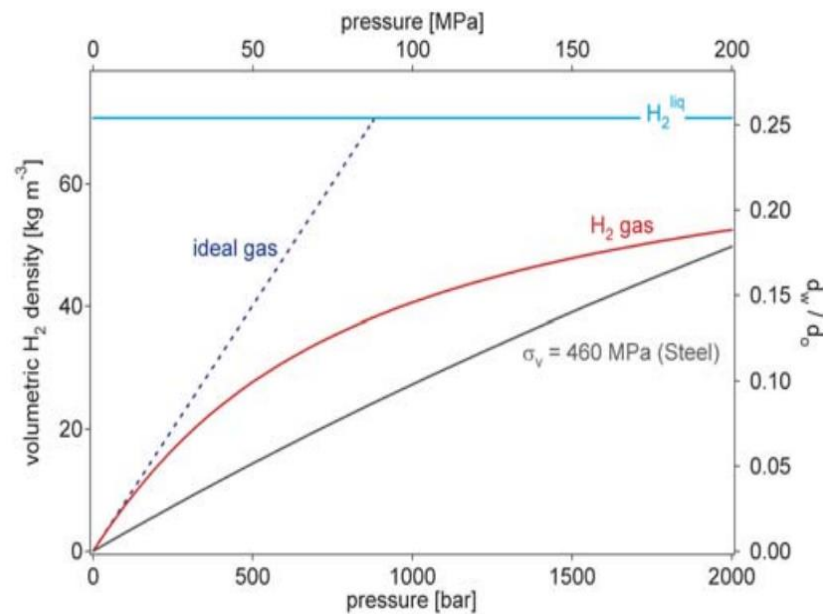


Figure 1.2: Volumetric density of compressed hydrogen gas as a function of gas pressure in comparison with the ideal gas and liquid hydrogen¹¹.

With the elevating gas pressure, the volumetric density of hydrogen gas also increases and it reaches the maximum at around 55 kg m^{-3} . Therefore, further increase of the hydrogen gas pressure does bring a little impact on the volumetric density of the compressed hydrogen gas. Moreover, huge amount of energy is required to achieve compression up to 700 bar for a reasonable driving range of 400-500 km¹⁷.

1.3.3 Hydrogen Storage in Solid Materials

As discussed earlier, hydrogen can be stored using solid materials through two different processes namely physisorption and chemisorption. Physisorption or so-called physical adsorption, is a process in which it involves the Van der Waals forces of attraction between the adsorbate and adsorbent. Like other gases, hydrogen adsorbs onto the surface of solid materials via weak Van der Waals force (1-10 kJ mol⁻¹ H₂). Since the force is weak, significant hydrogen physisorption can only be detected at low temperatures. Thus, liquid nitrogen, with a boiling point of 77 K is commonly used as a coolant to maximize this interaction. Materials available today for hydrogen storage via physisorption is controlled by specific surface area and pore sizes. As such, solids with high surface area for instances, zeolites¹⁸, activated carbons¹⁹ and metal-organic frameworks (MOFs)²⁰⁻²¹ are common materials for hydrogen storage. Moreover, Zhang in 2003 claimed that the amount of adsorbed hydrogen on the storage materials is directly proportional to the BET surface area or so-called total surface area based on the multipoint Brunauer, Emmett and Teller method of the materials at low temperatures²².

On the other hand, chemisorption (chemical adsorption) is a kind of adsorption in which the hydrogen undergoes chemical reaction with the solid materials to form new compounds. Although it possesses higher storage densities, the existence of strong chemical bond between the atoms makes the bond dissociation energy intensive. Henceforth, the reaction enthalpy involved in this chemisorption is definitely higher than that in physisorption. The materials which store the hydrogen via chemisorption are metal hydrides, complex hydrides, chemical hydrides and organic hydrides. Figure 1.3 below exhibits how hydrogen store through physisorption and chemisorption. Apparently, storing hydrogen via chemical

adsorption involved the breakage of H-H bond so that the hydrogen atom is stored interstitially in the solid materials.

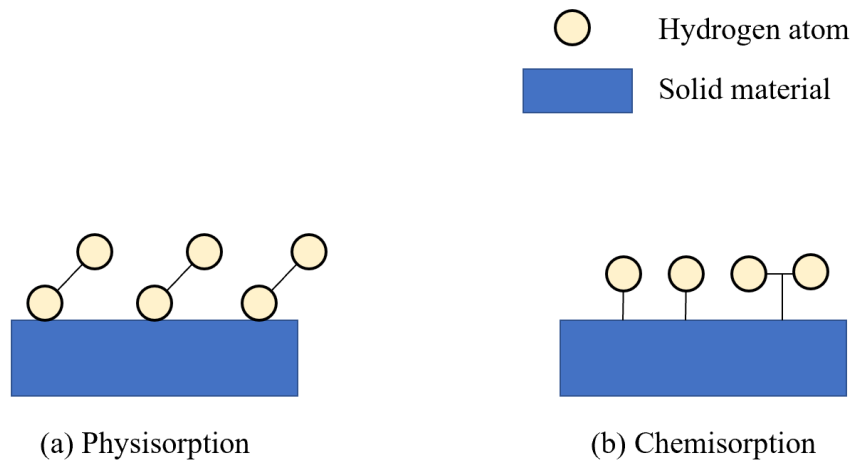


Figure 1.3: (a) Physisorption and (b) chemisorption of hydrogen on solid materials.

Table 1.3 summarizes the comparison between physisorption and chemisorption. Both physisorption and chemisorption exert Van der Waals force and chemical bond, respectively. The enthalpy of physisorption is relatively low, which is approximately $10\text{-}40\text{ kJ mol}^{-1}$ whereas the chemisorption demonstrates higher reaction enthalpy in the range of $20\text{-}400\text{ kJ mol}^{-1}$. Moreover, physisorption is a reversible process as desorption of adsorbate happens by lowering the activity of the adsorptive in the fluid surrounding the surface. In additions, an activation energy is also required in chemisorption to break the bond between hydrogen atoms (such as temperature, pressure and etc.) but physisorption does not hold any activation energy as the hydrogen molecules are adsorbed on the surface of the host materials. As such, physisorption is an instantaneous process whereas chemisorption requires certain conditions to make the process favourable.

Table 1.3: Comparison between physisorption and chemisorption from various aspects.

Physisorption	Aspects	Chemisorption
Van der Waals force	Types of interaction	Chemical bond
No	Specific	Yes
Low	Enthalpy of adsorption	High
Low	Temperature	High
No	Activation energy	Yes (high)
Instantaneous	Process	Slow

1.4 Hydrogen Storage in Malaysia

The depletion of fossil fuels for the global energy demand has become a hot topic for discussion lately. Because of this, Malaysia has reacted to the globally anticipated energy security crisis and climate change by enlarging fuel-resources to comprise renewable and alternative energy, thus developing green-energy technologies in coming decades. Substituting the current fossil fuels with hydrogen gas, is an advanced green technology that has the prospective to lead a clean and free emission energy for sustainable development objective. Hydrogen is not an energy source but a secondary energy carrier that can be produced from naturally available resources. In conjunction with the development of alternative renewable sources of energy for the economy, the developing countries such as China has acknowledged the importance of hydrogen energy and aspires to replace past conventional unsustainable vehicle technology with hydrogen fuel cell technology by aiming Research and Development (R&D) towards hydrogen energy as an advanced green technology⁹. In Malaysia, research on renewable energy has been focused by the Ministry of Science, Technology and Innovation (MOSTI) lately. Henceforth, hydrogen energy which falls within the scope of renewable energy has received significant research attention from the research community in Malaysia.

Undeniably, with an efficient hydrogen storage system, it is possible to develop a reversible on-board hydrogen storage system for fuel cell vehicle. In

Malaysia, transportation sector is emerging as the leading energy consuming sector since 2011. From this, Malaysia has reviewed the significance in taking the same R&D initiative on fuel cells due to the fact that the momentum for CO₂ emission is expected to dominate in these regions. Furthermore, in order to attain the Conference of Parties 21 (COP 21) commitment, in 2030, 45% reduction on the emission of greenhouse gases should be achieved in the transportation sector to make sure long term energy security²³. As such, the development of hydrogen energy system and fuel cells in Malaysia are urgently needed. It is believable that with the advancement of hydrogen storage research, implementation of hydrogen energy in Malaysia is thus highly possible.

1.5 Problem Statement

In the past, tremendous research efforts have devoted on the development of inorganic hydrides such as alanates²⁴, amide-hydride composites²⁵, borohydrides²⁶ and etc. With regards to organic hydrides, less attention has been committed²⁷⁻²⁸, undervaluing the potential of the large family of organic compounds. This is probably due to the difficulties in manipulating the thermodynamic properties and the selectivity in the dehydrogenation of organic hydrides. Previous studies have reported several approaches to tune the enthalpy of dehydrogenation, such as incorporation of heteroatoms (nitrogen or oxygen atom) to the aromatic ring, addition of electron donating substituent such as alkyl group to the ring to achieve enhanced aromatic stabilization. However, the addition of heavy alkyl group would inevitable scarify the hydrogen storage capacity of the material. In view of the strong electron donating nature of metal cations, in this project, we mainly focused on three parent organic substituents (pyrrole, imidazole and carbazole) by replacing the hydrogen of amine group with more electropositive alkali or alkaline earth metal

cations in order to change the polarity and intermolecular interactions. We believe that through this attempt, the dehydrogenation properties of these substances can be improved significantly.

1.6 Research Objectives

In this research project, we aim to achieve the following targets:

- i. To synthesize and structurally characterize metallo-N-heterocycles as novel hydrogen storage materials.
- ii. To study the catalytic hydrogenation and dehydrogenation of metallo-N-heterocycles using volumetric release measurement and Nuclear Magnetic Resonance Spectroscopy (NMR).
- iii. To investigate the hydrogen storage reversibility of the newly developed metallo-N-heterocycles.

CHAPTER 2

LITERATURE REVIEW

2.1 Physisorption Hydrogen Storage Materials

In 1997, Dillon et al. first reported the hydrogen storage properties of carbon nanotubes²⁹. Upon this invention, a series of carbon-based hydrogen storage materials such as carbon materials, mesoporous materials and etc were studied both intensively and extensively³⁰⁻³¹. Since physical adsorption relies on the weak van der Waals interaction between the materials and hydrogen gas molecules during the storage, therefore, activation of the materials are not required. At the same time, the fast hydrogen absorption and desorption rate as well as good reversibility of this material are suitable for reversible hydrogen storage. Nevertheless, the weak van der Waals interaction ($3-6 \text{ kJ mol}^{-1}$) requires hydrogen absorption to occur at low temperatures. Intense investigations have proven that there is no significant difference of the hydrogen storage performance of carbon nanotubes, fullerenes, carbon nanofibers and other nanostructured carbon materials as compared to activated carbon³²⁻³³. At $-196 \text{ }^\circ\text{C}$, the highest gravimetric capacity is approximately 4 wt% whereas at room temperature, the storage capacity is less than 1 wt%. As such, it can be concluded that the hydrogen storage capacity is proportional to the micropore volume of the carbon materials³⁴⁻³⁶. From this point of view, the theoretical hydrogen storage capacity of carbon materials do not exceed 6.5 wt% (with the micropore of $0.92 \text{ cm}^3 \text{ g}^{-1}$)³⁶.

After several years of workout, Yaghi and coworkers²⁰ proposed another physisorption material which is metal organic framework (MOF) using $\text{Zn}_4\text{O}(\text{BDC})_3$ material. According to their study, $\text{Zn}_4\text{O}(\text{BDC})_3$ was capable to exhibit 4.5 wt% of volumetric capacity at temperature as low as 78 K, which shows a huge improvement

in the development of physisorption materials. As reported, MOFs received vast attentions and significances until they are the most invented candidates in hydrogen storage applications owing to their high specific area (even higher than $5000 \text{ m}^2 \text{ g}^{-1}$) and uniform microporous structure (with diameter $0.5\text{-}2 \text{ nm}$)^{32-33, 37}. In comparison with carbon-based materials, most of the MOFs also fulfill the gravimetric capacity and material surface area together with the microporous volume relationships. Till now, many MOFs have been reported such as MOF-5, IRMOF-20, MOF-1777 in which the hydrogen capacity of each materials has achieved 5.2 wt% (48 bar), 6.7 wt% (70 bar) and 7.5 wt% (70 bar), respectively, at $-196 \text{ }^\circ\text{C}$. Nevertheless, their capacity still could not even reach 1.5 wt% upon temperature at $25 \text{ }^\circ\text{C}$ ³⁸. Because of this problem, Van der Berg and Areal³³ suggested that by tailoring the enthalpy of hydrogen adsorption, the hydrogen physisorption properties could be enhanced. Long et al.³⁹⁻⁴⁰ in 2005 successfully tailored the enthalpy change of hydrogen adsorption from the range of -3.5 to $-6.5 \text{ kJ mol}^{-1}\text{-H}_2$ to the range of -9.5 to $-10.1 \text{ kJ mol}^{-1}\text{-H}_2$ via the introduction of exposed Mn^{2+} or Mg^{2+} coordination site into the MOFs. Other than that, Zhao and Chen also claimed that by reducing the pore diameter of the materials to the diameter smaller than hydrogen molecules (2.9 \AA) can also increase the hydrogen absorption and desorption operating temperature⁴¹⁻⁴². Despite the relatively low operating temperature of hydrogen adsorption and desorption, low volumetric hydrogen storage density may account for the limitation of physisorption materials to be applied in hydrogen storage. For an example, the volumetric hydrogen storage density of MOF-177 is 32 kg cm^{-3} ³⁸ but this value is still far away from the DOE target in 2010 which is 45 kg cm^{-3} . Although physisorption material is currently encountering problems as mentioned above, it is still regarded as one of the promising materials which is worth for further investigation as it paves the way to

overcome the shortcomings of low temperature liquid hydrogen storage technology³²⁻

33

2.2 Chemisorption Hydrogen Storage Materials

2.2.1 Metal Hydrides

Since the late 1960s, research focused on metal hydrides as hydrogen storage materials have been studied both intensively and extensively and most of these materials remain stable at atmospheric pressure⁴³⁻⁴⁴. Generally, the formations of metal hydrides between metals and hydrogen are exothermic processes and the process is reversible. In order to stimulate the liberation of hydrogen from these materials, an optimum temperature or reduced pressure is required. Metal hydrides are grouped into several categories such as AB₅, AB₃, AB₂, AB and A₂B. Among the listed metal hydrides, element A always resembles the rare metals or alkaline earth metals that forms stable hydride compounds easily with hydrogen whilst element B usually consists of transition metals that causes the formation of unstable metal hydrides upon the reaction with hydrogen. Hydrogen is basically stored in the form of atoms in the lattice or gap of these alloys and most of the metal alloys can reversibly store hydrogen as described in Equation 2.1⁴⁴.



The reversible absorption and desorption of hydrogen storage materials is usually controlled by its thermodynamic conditions. Therefore, this condition can be described using a pressure-concentration-isothermal (PCI) curve (Figure 2.1)⁴⁵. Upon the pressure platform measurement at different temperatures, followed by the combination with van't Hoff equation (Equation 2.2), both the enthalpy (ΔH) and entropy change (ΔS) of the materials from the reversible hydrogen absorption and desorption process can be obtained. The van't Hoff equation represented below,

where P is the equilibrium pressure, P° is a reference pressure at atmospheric pressure, R is the gas constant, T is the absolute temperature, and ΔH and ΔS are the enthalpy change and entropy change, respectively that involved in the formation of metal hydrides.

$$\ln \frac{P}{P^\circ} = -\frac{\Delta H}{RT} + \frac{\Delta S}{R} \quad (2.2)$$

LaNi_5 and Mg_2Ni are two commonly known metal hydrides. LaNi_5 recorded the hydrogen content of approximately 1.4 wt% and a hydrogen equilibrium pressure of 2 bars at room temperature⁴⁶ whereas Mg_2Ni revealed approximately 3.6 wt% with a hydrogen equilibrium pressure of 1 bar at 282 °C/ 555 K⁴⁷. Because of their relatively low weight density, appropriate reversibility and recyclability of hydrogen, metal hydrides are propitious for stationary applications. Nevertheless, due to the significant attention has been given to mobile applications lately, research efforts using metal hydrides have been moved to lighter and cheaper metal hydrides such as LiH and MgH_2 , which are two well-known simple binary hydrides, owing to their high hydrogen capacities (LiH : ~12.5 wt%, MgH_2 : ~7.7 wt%)⁴⁸. In spite of that, both LiH and MgH_2 are very stable, in order to release 1 bar of equilibrium pressure, 910 °C and 277 °C are needed, respectively. The high decomposition temperature of LiH has constrained it for practical applications. As such, much attention has been devoted to MgH_2 due to its thermodynamic property which is somehow better than LiH .

Although MgH_2 exhibits a better thermodynamic property than LiH , it still suffers from slow dehydrogenation kinetics. Henceforth, recent work mainly focus on the chemical compositional alterations and catalytic improvements of MgH_2 . To illustrate, the addition of transition metals (Ti, Nb, V, Mn, Fe, Co and Ni) and some of their oxides of metal have improved the dehydrogenation kinetics of MgH_2

substantially⁴⁹⁻⁵². More interestingly, Hanada et al. reported the finding of nano-sized Ni-doped MgH₂ revealed 6.5 wt% of hydrogen capacity at 150-200 °C⁵¹. Notwithstanding the fact that doping of Ni had apparently altered the kinetics but not the thermodynamic of MgH₂. Until recently, Zhou and coworkers⁵³ proclaimed the addition of In into the solid MgH₂ showed thermodynamic improvement upon the formation of MgIn solid solution. By increasing 10% of molar ratio of In, the enthalpy of dehydrogenation decreased from 76.6 kJ mol⁻¹-H₂ to 70.9 kJ mol⁻¹-H₂.

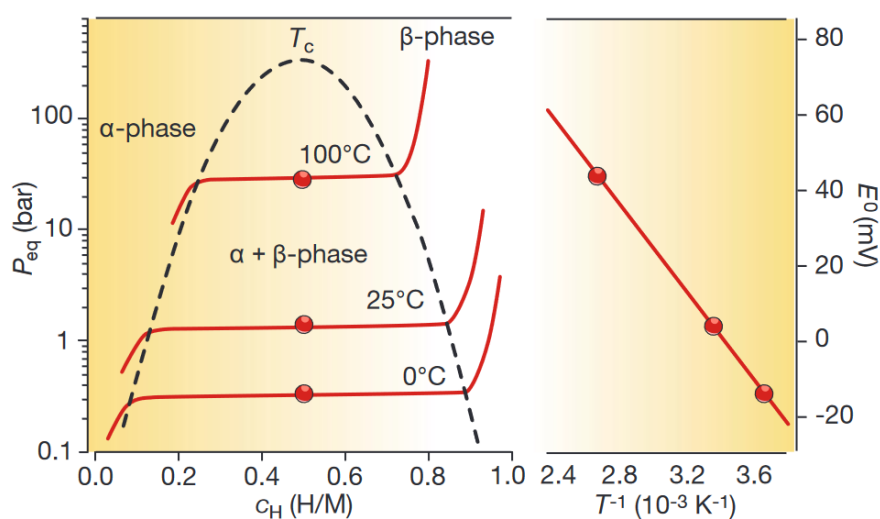


Figure 2.1: Pressure-concentration-temperature plot and a van't Hoff curve⁴⁵.

2.2.2 Alanates

Previously, the study of complex aluminium hydrides as hydrogen storage materials were sparse until an impressive improvement on tailoring the dehydrogenation properties of NaAlH₄ was conducted by Bogdanovic and Schwickardi in 1997 via the incorporation of NaAlH₄ with TiCl₃²⁴. Upon this approach, the dehydrogenation temperature (~80 °C) of NaAlH₄ was significantly reduced²⁴. Among the aluminium hydrides, NaAlH₄ was the well-studied compound, owing to its 7.4 wt% of hydrogen content. Besides, Ti-doped NaAlH₄ also revealed long-term cycling behaviour, by which after 100 cycles were conducted, the

hydrogen capacity still attained more than 3 wt%⁵⁴. It should be noted that the dehydrogenation of NaAlH₄ is a step-wise reaction and is accompanied by phase transformations. In 1970s, Dilts et al.⁵⁵ studied the thermal decomposition of NaAlH₄ extensively. According to their findings, NaAlH₄ was first melted at 165 °C–205 °C, followed by the liberation of *ca.* 3.7 wt% of hydrogen via endothermic reaction to become Na₃AlH₆ (Equation 2.3). Subsequently, at 250 °C–300 °C, an endothermic reaction also took place in which Na₃AlH₆ released *ca.* 1.8 wt% hydrogen (Equation 2.4), together with the formation of Al and NaH. Beyond 450 °C, NaH decomposed to release hydrogen (Equation 2.5)⁵⁵⁻⁵⁶. However, because of the decomposition of NaH to metallic Na in the final stage to evolve H₂ involved relatively high temperature, only the emission of H₂ from the first and second stage in the thermal decomposition of NaAlH₄ (5.4 wt%) are regarded useful for hydrogen storage purpose⁵⁵.



Another well-known complex aluminium hydride, LiAlH₄ has also received significant attention in the past because of its high hydrogen capacity (10.6 wt%). Both the aluminium hydride of sodium and lithium decompose in the same manner, in which step-wise reaction is involved. Initially, LiAlH₄ melted at temperature 165 °C–175 °C and decomposed exothermally at 165 °C–175 °C to obtain Li₃AlH₆, Al and 5.3 wt% of hydrogen (Equation 2.6). After this, Li₃AlH₆ further decomposed endothermically to release *ca.* 2.7 wt% of hydrogen (Equation 2.7). At higher temperatures (370 °C–483 °C), LiH dissociated into lithium metal and 2.7 wt% of hydrogen (Equation 2.8)^{55, 57}.



Because the first step of decomposition of LiAlH_4 is an exothermic reaction, therefore, rehydrogenation of Li_3AlH_6 - 2Al back to LiAlH_4 is impossible. Table 2.1 below exhibits several examples of complex aluminium hydrides as hydrogen storage materials. Their thermodynamic or kinetic limitations have restricted their applications as on-board hydrogen storage materials.

Table 2.1: Physical constants of selected complex aluminium hydrides.

Compound	Decomposition temperature (°C)	Hydrogen capacity (wt%)	Ref.
KAlH_4	>300	5.8	58
$\text{Mg}(\text{AlH}_4)_2$	110-130	9.3	59
$\text{Ca}(\text{AlH}_4)_2$	80	7.9	60
$\text{LiMg}(\text{AlH}_4)_3$	120	9.7	60
LiMgAlH_6	170	9.4	60

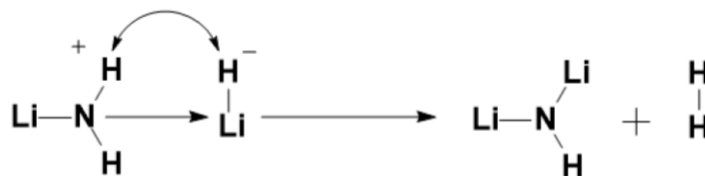
2.2.3 Amide-Hydride Interaction

Nitrogen-metal complex hydrides have rarely been concerned especially as hydrogen storage materials. Until Chen et al.²⁵ in 2002 reported the amide-hydride interaction via the discovery of hydrogenation of Li_3N , it has triggered the worldwide researchers to focus on the development of nitrogen-containing metal hydrides as potential hydrogen storage materials. Li_3N was capable to reversibly store enormous amount of hydrogen (~10.5 wt%) in stepwise process, forming Li_2NH as intermediate and LiNH_2 and LiH as products (Equation 2.9). Interestingly, Li_2NH alone can also reversibly absorb 6.5 wt% of hydrogen.



Further mechanistic investigation proved that this interaction typically involved the two oppositely charged of protic ($\text{H}^{\delta+}$) and hydridic ($\text{H}^{\delta-}$) hydrogen,⁶¹ in

which the $H^{\delta+}$ is from amide whereas the $H^{\delta-}$ is from hydride (Scheme 2.1). The combination of both these $H^{\delta+}$ and $H^{\delta-}$ between the metal cation and nitrogen group induce a direct interaction to form hydrogen.



Scheme 2.1: Interaction between lithium amide and lithium hydride to form lithium imide and H_2 .

Motivated by the successful attempts in storing considerable amount of H_2 in Li-N-H system, researchers further invented a series of amide-hydride hydrogen storage system using different metal cations pairs, such as binary M-N-H system ($Mg(NH_2)_2$ - MgH_2 ⁶²⁻⁶³ and $Ca(NH_2)_2$ - CaH_2 ⁶⁴). As reported by Ichikawa et al.⁶⁵ in 2004, the thermodynamic reversible hydrogenation and dehydrogenation properties of Li-N-H can be improved to a better stage via the introduction of additives ($TiCl_3$ and Li_2O). In addition, further exploration of ternary M_1 - M_2 -N-H system, for instances, $LiNH_2$ - CaH_2 ,⁶⁶ $Mg(NH_2)_2$ - LiH ,⁶⁶⁻⁶⁸ $Mg(NH_2)_2$ - NaH ,⁶⁹ $Ca(NH_2)_2$ - NaH ⁷⁰ and others could even reduce the dehydrogenation temperature and pressure of Li-N-H system, which is suitable for practical application purposes. Among the systems proposed, Li-Mg-N-H⁷¹⁻⁷² is currently the most suitable hydrogen storage system, with a hydrogen capacity of 5.4 wt% when the temperature reached 180 °C (Figure 2.2).

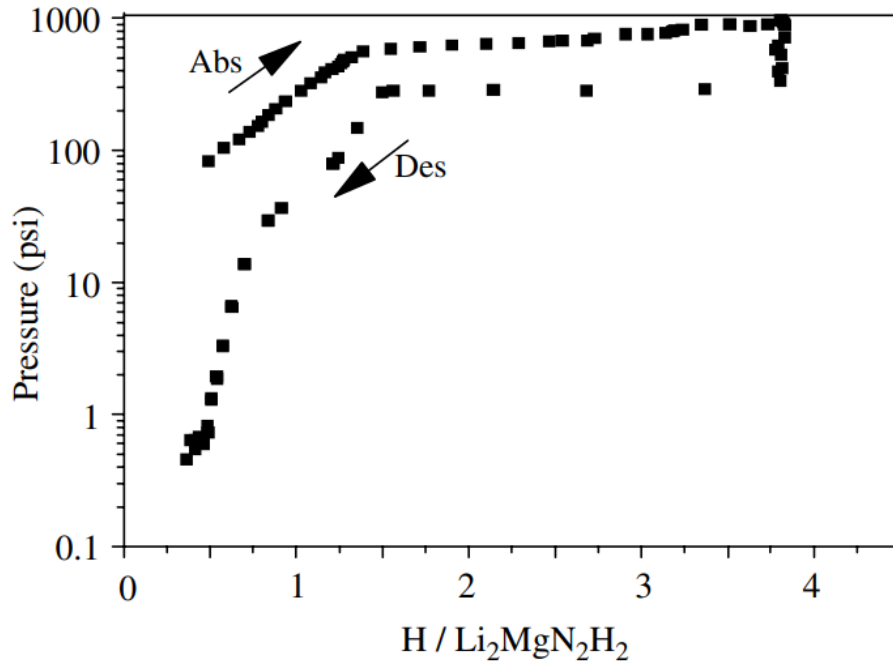


Figure 2.2: PCT curve of $\text{Li}_2\text{Mg}(\text{NH})_2$ at $180\text{ }^\circ\text{C}$ ^{66,72}.

Empirically, upon hydrogenation, metal nitride will convert into a mixture of several components such as metal imide, metal amide or metal hydride. Therefore, a slight modification of these compounds by partially or completely replacing the above components with different metal amides or metal hydrides, a series of new hydrogen storage systems can be derived. Only few years of exploration, nitrogen-containing metal hydrides hydrogen storage materials have developed into a big family of system which include binary system, ternary system and complex system. Binary system is defined as a system which consists of only single metal in a metal-N-H compound. Metal-N-H compounds with more than two or three metal atoms are known as ternary or multicomponent systems. Table 2.2 summarizes the chemical reaction of metal-N-H hydrogen storage systems.

Table 2.2: Summary of the chemical reactions of metal-N-H hydrogen storage systems.

Reaction System	Chemical Equations	Equation	Theoretical Gravimetric Capacity (wt%)	Ref.
Binary System	$\text{LiNH}_2 + 2\text{LiH} \leftrightarrow \text{Li}_2\text{NH} + \text{LiH} + \text{H}_2$	2.15	6.5	25, 73-75
	$\text{LiNH}_2 + 2\text{LiH} \leftrightarrow \text{Li}_3\text{N} + 2\text{H}_2$	2.16	10.3	
	$\text{Mg}(\text{NH}_2)_2 + 2\text{MgH}_2 \leftrightarrow 2\text{MgNH} + \text{MgH}_2 + 2\text{H}_2$	2.17	4.9	76-78
	$\text{Mg}(\text{NH}_2)_2 + 2\text{MgH}_2 \leftrightarrow \text{Mg}_3\text{N}_2 + 4\text{H}_2$	2.18	7.4	
	$\text{CaNH} + \text{CaH}_2 \leftrightarrow \text{Ca}_2\text{NH} + \text{H}_2$	2.19	2.1	25, 79-80
	$\text{Ca}_3\text{N}_2 + 2\text{H}_2 \rightarrow 2\text{CaNH} + \text{CaH}_2 \leftrightarrow \text{Ca}_2\text{NH} + \text{CaNH} + \text{H}_2$	2.20	2.1	
	$\text{Ca}(\text{NH}_2)_2 + 3\text{CaH}_2 \rightarrow 2\text{CaNH} + 2\text{CaH}_2 + 2\text{H}_2 \leftrightarrow 2\text{Ca}_2\text{NH} + 4\text{H}_2$	2.21	2.1	
Ternary System	$2\text{LiNH}_2 + \text{MgH}_2 \rightarrow \text{Mg}(\text{NH}_2)_2 + 2\text{LiH} \leftrightarrow \text{Li}_2\text{Mg}(\text{NH})_2 + 2\text{H}_2$	2.22	5.6	66, 81-88
	$3\text{Mg}(\text{NH}_2)_2 + 8\text{LiH} \leftrightarrow \text{Mg}_3\text{N}_2 + 4\text{Li}_2\text{NH} + 8\text{H}_2$	2.23	6.9	
	$3\text{Mg}(\text{NH}_2)_2 + 12\text{LiH} \leftrightarrow \text{Mg}_3\text{N}_2 + 4\text{Li}_3\text{N} + 12\text{H}_2$	2.24	9.1	
	$2\text{LiNH}_2 + \text{CaH}_2 \rightarrow \text{Li}_2\text{NH} + \text{CaNH} \rightarrow \text{Li}_2\text{Ca}(\text{NH})_2 + 2\text{H}_2$	2.25	4.6	66, 89-91
	$2\text{Ca}(\text{NH}_2)_2 + 2\text{LiH} \rightarrow \text{Li}_2\text{NH} + \text{CaNH} \rightarrow \text{Li}_2\text{Ca}(\text{NH})_2 + 2\text{H}_2$	2.26	4.6	
	$\text{Li}_2\text{Ca}(\text{NH})_2 + \text{H}_2 \leftrightarrow \text{LiNH}_2 + \text{CaNH} + \text{LiH}$	2.27	2.3	
	$2\text{Mg}(\text{NH}_2)_2 + 3\text{NaH} \leftrightarrow \text{'unknown phase'} + 2\text{H}_2$	2.28	2.2	
	$\text{Mg}(\text{NH}_2)_2 + \text{CaH}_2 \rightarrow \text{MgCa}(\text{NH})_2 + 2\text{H}_2$	2.29	4.1	93-94
	$\text{Ca}(\text{NH}_2)_2 + \text{NaH} \leftrightarrow \text{NaNH}_2 + \text{Ca-N-H solid solution} + 1/2\text{H}_2$	2.30	1.0	95
	Multicomponent System	$2\text{LiNH}_2 + \text{LiBH}_4 \rightarrow \text{Li}_3\text{BN}_2 + 4\text{H}_2$	2.31	11.9
$2\text{LiNH}_2 + \text{LiAlH}_4 \rightarrow \text{Li}_3\text{AlN}_2 + 4\text{H}_2$		2.32	9.6	98-102
$\text{Li}_3\text{AlN}_2 + 2\text{H}_2 \leftrightarrow \text{LiNH}_2 + \text{LiH} + \text{AlN}$		2.33	5.0	
$4\text{LiNH}_2 + 2\text{Li}_3\text{AlH}_6 \rightarrow \text{Li}_3\text{AlN}_2 + \text{Al} + 2\text{Li}_2\text{NH} + 2\text{LiH} + 15/2\text{H}_2$		2.34	7.6	
$\text{NaNH}_2 + \text{LiAlH}_4 \rightarrow \text{NaH} + 0.67\text{Al} + \text{LiAl}_{0.33}\text{NH} + 2\text{H}_2$		2.35	5.2	103
$3\text{Mg}(\text{NH}_2)_2 + 3\text{LiAlH}_4 \rightarrow \text{Mg}_3\text{N}_2 + \text{Li}_3\text{AlN}_2 + 2\text{AlN} + 12\text{H}_2$		2.36	8.5	104

2.2.4 Borohydrides

Schesinger et al.¹⁰⁵ consecutively prepared a series of metal borohydrides such as $\text{Al}(\text{BH}_4)_3$, NaBH_4 and KBH_4 , but these materials in the early stage were only utilized for the reduction of organic compounds. As we know, most of the borohydrides contain high hydrogen capacity, for instances, the hydrogen storage capacity of $\text{Be}(\text{BH}_4)_2$ is as high as 20 wt%. However, Be is highly toxic and therefore is not further explored as a hydrogen storage material. Furthermore, LiBH_4 and $\text{Mg}(\text{BH}_4)_2$ ¹⁰⁶⁻¹⁰⁷ can only release hydrogen at temperature more than 300 °C while $\text{Ca}(\text{BH}_4)_2$ ¹⁰⁸ started to desorb hydrogen at temperature higher than 350 °C. The high stability and the resulting high temperature for dehydrogenation make borohydrides impractical for hydrogen storage. To tackle these problems, intensive investigations have been reported to alter the dehydrogenation thermodynamic properties such as via the addition of catalysts, hydrides and amino compounds.

2.2.5 Ammonia Borane and Metal Amidoboranes

Ammonia borane, or denoted as AB, with its molecular formula NH_3BH_3 has a high gravimetric storage capacity of 19.6 wt% and $145 \text{ kg H}_2 \text{ L}^{-1}$, which is higher than the DOE target of mobile applications in 2015 (5.5 wt%; $40 \text{ g H}_2 \text{ L}^{-1}$). This material has been a hot topic of research in the past decades as a potential hydrogen storage candidate. Its first synthesis was reported by both Shore and Parry in 1955¹⁰⁹. At low temperature, AB is a tetragonal colourless crystal structure, with a space group of $I4mm$ (see Figure 2.3)¹¹⁰⁻¹¹¹. It exhibits high stability in both air and moisture. However, AB revealed several restrictions that limit its practical application as hydrogen storage material, for instances, the irreversible hydrogen release, high temperature for dehydrogenation and emission of unfavourable by-products during the dehydrogenation.

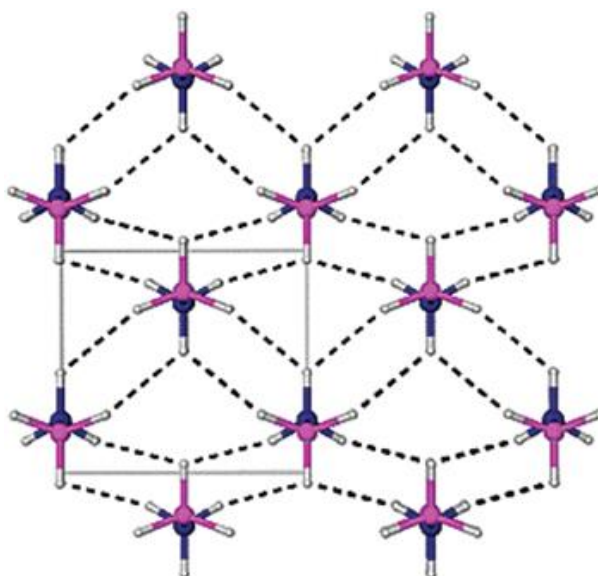


Figure 2.3: Crystal structure of ammonia borane¹¹¹.

Empirically, the thermal decompositions of AB are mainly divided into three steps as listed in Equation 2.10 to 2.12. In the first step, AB decomposed at 110 °C to generate an amorphous white powder of $(\text{NH}_2\text{BH}_2)_n$ (Equation 2.10). This NH_2BH_2 however further decomposed to polyiminoborane to release another equivalent of hydrogen at temperature above 150 °C. The final stage of the decomposition of AB occurred at temperature beyond 500 °C, to give BN and 1 equivalent hydrogen¹¹². Because the temperature required for Equation 2.12 is relatively high, thus only the hydrogen liberation in step 1 and step 2 are usable.



To date, numerous approaches had been employed to improve the dehydrogenation properties of AB, which include the addition of catalyst using transition metal nanoparticles (Ni, Fe, Ru, Tr, Pt), metal organic compounds¹¹³⁻¹¹⁴ or Lewis acid¹¹⁵ catalysts, nanoconfinement of AB molecules in mesoporous materials

such as SBA-15,¹¹⁶ MCM-41, carbon aerogel and chemical modification of AB molecules using alkali or alkaline earth metal to form metal amidoborane¹¹⁷⁻¹¹⁸.

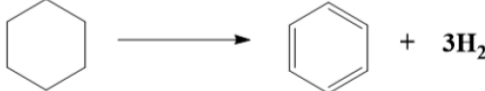
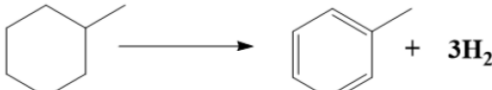
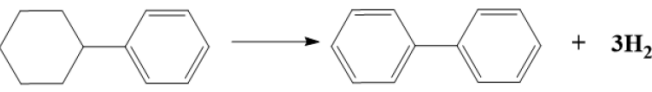
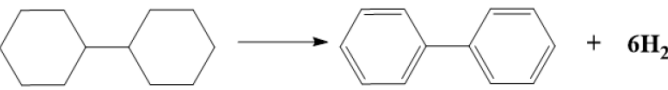
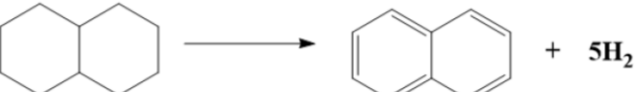
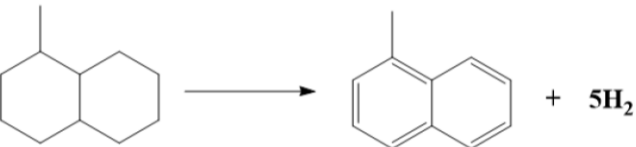
2.2.6 Organic Hydrides

Intensive efforts had been devoted on developing inorganic compounds for hydrogen storage until Sultan addressed the strategic on Liquid Organic Hydrogen Carriers (LOHCs) technology in 1975¹¹⁹. Hydrogen can be reversibly stored in organic molecules via hydrogenation and dehydrogenation. In additions, adopting LOHCs as hydrogen energy carriers possess several advantages:

- Absence of greenhouse gases (CO, CO₂) and other side products,
- High gravimetric hydrogen storage capacity (5-8 wt%),
- Integrate with the present infrastructures with minimal modification, and
- Total catalytic reversible reaction.

Organic compounds, in particular, toluene¹²⁰, dibenzene toluene¹²¹⁻¹²², formic acid¹²³⁻¹²⁴, alcohols¹²⁵⁻¹²⁶ and carbohydrates¹²⁷⁻¹²⁹ have been studied intensively and extensively, nonetheless, these organic hydrides did not receive much attention because the emission of H₂ is a strongly endothermic process ($\Delta H_d = 60-70 \text{ kJ mol}^{-1}\text{-H}_2$)¹³⁰⁻¹³¹. Table 2.3 exhibits various potential cycloalkanes with their volumetric capacity and enthalpy of dehydrogenation. It can be clearly seen that the enthalpy values are relatively high. Henceforth, high temperatures are required for dehydrogenation to occur. Taking methylcyclohexane as an instance, the calculated ΔH_d is approximately $\sim 73.6 \text{ kJ mol}^{-1}\text{-H}_2$. Thus, even with the aid of a suitable catalyst, the dehydrogenation can only be initiated at a temperature of 300 °C¹³². Hence, researches focus not only on developing high efficiency hydrogenation and dehydrogenation catalysts¹³³⁻¹³⁶ but also synthesizing new aromatic organic hydrides¹³⁷ for hydrogen storage.

Table 2.3: Examples of different cycloalkanes with their enthalpies of dehydrogenation¹³⁸.

Reaction scheme	H° (kJ mol ⁻¹ -H ₂)
	+68.6
	+68.3
	+65.9
	+66.6
	+64.0
	+66.7

To overcome these barriers, Pez et al. initiated the finding by conducting a series of systematic theoretical screening of LOHC candidates involving N-heteroaromatics and it was found that the presence of heteroatoms (N atom) into the carbon rings^{27-28, 139} or substitution of a more electron donating group outside the ring¹⁴⁰ would alter the thermodynamics of dehydrogenation efficiently (Table 2.4).